

# The properties of the stellar populations in ULIRGs II: star formation histories and evolution

J.Rodríguez Zaurín<sup>1,2\*</sup>, C.N Tadhunter<sup>2</sup> and R.M.González Delgado<sup>3</sup>

<sup>1</sup>Department of molecular and infrared astronomy, IEM (CSIC), 28006 Madrid, SPAIN

<sup>2</sup>Department of physics and Astronomy, University of Sheffield, Sheffield S3 7RH

<sup>3</sup>Instituto de Astrofísica de Andalucía(CSIC), P.O.Box 3004, 18080 Granada, Spain

8 October 2018

## ABSTRACT

This is the second of two papers presenting a detailed long-slit spectroscopic study of the stellar populations in a sample of 36 ULIRGs. In the previous paper we presented the sample, the data and the spectral synthesis modelling. In this paper we carry out a more detailed analysis of the modelling results, with the aim of investigating the general properties of the stellar populations (i.e. age, reddening and percentage contribution) and the evolution of the host galaxies, comparing the results with other studies of ULIRGs and star forming galaxies in the high- $z$  Universe. The characteristic age of the young stellar populations (YSPs) is  $\leq 100$  Myr in the nuclei of the overwhelming majority of galaxies, consistent with the characteristic timescale of the major burst of star formation associated with the final stages of major galaxy mergers. However, the modelling results clearly reveal that the star formation histories of ULIRGs are complex, with at least two epochs of star formation activity. Overall, these results are consistent with models that predict an epoch of enhanced star formation coinciding with the first pass of the merging nuclei, along with a further, more intense, episode of star formation occurring as the nuclei finally merge together. It is also found that, although YSPs make a major contribution to the optical emission in most of the extended and nuclear apertures examined, they tend to be younger and more reddened in the nuclear regions of the galaxies. This is in good agreement with the merger simulations, which predict that the bulk of the star formation activity in the final stages of mergers will occur in the nuclear regions of the merging galaxies. In addition, our results show that ULIRGs have total stellar masses that are similar to, or smaller than, the break of the galaxy mass function (i.e. ULIRGs are sub- $m_*$  or  $\sim m_*$  systems), and that the young stellar populations detected at optical wavelengths dominate the stellar mass contents of the galaxies. Finally, we find no significant differences between the ages of the YSP in ULIRGs with and without optically detected Seyfert nuclei, nor between those with warm and cool mid- to far-IR colours. While this results do not entirely rule out the idea that cool ULIRGs with HII/LINER spectra evolve into warm ULIRGs with Seyfert-like spectra, it is clear that the AGN activity in local Seyfert-like ULIRGs has not been triggered a substantial period ( $\geq 100$  Myr) *after* the major merger-induced starbursts in the nuclear regions.

**Key words:** Galaxies: evolution – galaxies: starburst.

## 1 INTRODUCTION

First discovered in large numbers by the *IRAS* satellite, ultraluminous infrared galaxies (ULIRGs,  $L_{\text{IR}} > 10^{12} L_{\odot}$ ) represent some of the most rapidly evolving objects in the local Universe. These objects are important in several respects,

such as testing the merger models, investigating the nature of the AGN-starburst connection in merging systems, and understanding the physical processes taking place in the recently discovered high-redshift star forming galaxies, which have similar properties to the nearby ULIRGs.

A remarkable property of ULIRGs is that more than 90% of them are associated with galaxy mergers and interactions (see Sanders & Mirabel, 1996, for a review). The

\* E-mail: jrzd@damir.iem.csic.es

simulations have shown that, during galaxy collisions involving gas-rich disk galaxies, the gas loses angular momentum due to dynamical friction, tidal torques, and inflows towards the centres of the galaxies (e.g. Mihos & Hernquist, 1996). Such high nuclear concentrations of gas are capable of triggering both starburst and AGN activity. In general, these simulations predict two epochs of enhanced star formation in major galaxy mergers: the first occurring around the first encounter, and the second episode when the nuclei are close to coalescence (Mihos & Hernquist, 1996; Barnes & Hernquist, 1996; Springel et al., 2005; Cox et al., 2006; di Matteo et al., 2007). However, both the time lag and the relative intensity of the peaks of starburst activity during the merger event depend on several factors, such as the presence of bulges, feedback effects, gas content and orbital geometry. Given that the models make specific predictions about the histories of the star formation triggered in the course of major gas-rich mergers, studies of the stellar populations in ULIRGs provide useful information about the mergers and, potentially, allow us to test the models.

ULIRGs are classified on the basis of their infrared colours as warm ( $f_{25}/f_{60} > 0.2$ )<sup>1</sup> and cool ( $f_{25}/f_{60} \leq 0.2$ ) ULIRGs. Warm ULIRGs represent  $\sim 20 - 25\%$  of the total population of ULIRGs discovered by *IRAS*. Most of such objects have an AGN optical spectral classification, tend to be more compact than cool ULIRGs, and are frequently found in an advanced merger state (Surace et al., 1998). These properties suggest that ULIRGs play an important role in the formation and evolution of QSOs (Sanders et al., 1988b) and radio galaxies (Tadhunter et al., 2005). Indeed, Sanders et al. (1988b) proposed a scenario in which cool ULIRGs evolve into warm ULIRGs on their way to becoming typical optically-selected QSOs. Further evidence in favour of such an evolutionary scenario was reported by Surace et al. (1998), Surace & Sanders (1999), Surace et al. (2000) and Surace & Sanders (2000) on the basis of their imaging studies of cool and warm ULIRGs, and Canalizo & Stockton (2000a,b, 2001), based on a spectroscopic analysis of a sample of transition QSOs — objects that, based on their infrared colors, may represent a transitional stage between ULIRGs and QSOs. More recently, Tadhunter et al. (2007) carried out a mid- to far-IR study of powerful radio galaxies, searching for signs of hidden star formation activity. They found that the fraction of powerful radio galaxies with energetically significant star formation activity (20% – 30%) is similar to that deduced from optical studies. The derived ages and masses of the young stellar populations in the Wills et al. (2004), Tadhunter et al. (2005) and Tadhunter et al. (2007) samples of radio galaxies, and the fact that some of these radio galaxies are actually classified as ULIRGs, is consistent with the idea that some radio galaxies are the evolved product of ULIRGs (Tadhunter et al., 2005).

In terms of the end products of the merger events associated with ULIRGs, the kinematic studies of Genzel et al. (2001) and Tacconi et al. (2002) have shown that ULIRGs match the locations of intermediate mass, disk ellipticals and S0 galaxies in the fundamental plane. ULIRGs have

effective radii and velocity dispersions smaller than those of their comparison sample of nearby radio galaxies. Furthermore, the dynamical masses of ULIRGs are  $10^{10} - 10^{11} M_{\odot}$  (Tacconi et al., 2002; Colina et al., 2005; Dasyra et al., 2006a,b), which is similar to intermediate-mass elliptical galaxies. Based on the dynamical properties of ULIRGs, Tacconi et al. (2002) concluded that not all ULIRGs can evolve into typical QSOs or powerful radio galaxies. However, the recent work of Dasyra et al. (2007), based on near-IR spectroscopic observations of a sample of 12 (mainly Palomar Green) QSOs, has shown that it is possible for ULIRGs to have similar dynamical properties to QSOs. Therefore, it is clear that, despite the recognition of an evolutionary link between ULIRGs, QSOs/radio galaxies and elliptical galaxies, considerable uncertainties remain about the true nature of the link.

Studies of ULIRGs are also important in the context of the various populations of high- $z$  galaxies that have been recently detected using near-IR (distant red galaxies, DRGs, Franx et al., 2003), mid-IR ( $24\mu\text{m}$  *Spitzer*-selected galaxies, Caputi et al., 2006; Yan et al., 2007; Sajina et al., 2007, and others), and sub-millimeter wavelengths (sub-mm galaxies, SMGs, Smail et al., 2002; Blain et al., 2002; Chapman et al., 2003; Pope et al., 2005, and others). These objects have properties similar to the nearby ULIRGs (stellar mass and luminosity, for example), and make up a substantial fraction of the star formation (SF) at  $z \sim 1-2$ . As local analogues of such objects, ULIRGs provide an opportunity to study the physical processes associated with their prodigious SF activity in depth.

It is also important to emphasize that most of the studies of the stellar populations in high redshift galaxies are based on the modelling of a few photometric points and, therefore, it is hard to constrain the properties of these populations. Sensitive studies of star forming galaxies at lower redshifts are useful, not only to better understand the links between local starburst objects and their high- $z$  counterparts, but also to gain valuable information on the uncertainties associated with the derived properties of the stellar populations in high- $z$  star forming galaxies.

At this stage it is clear that there are many unresolved issues concerning the nature of ULIRGs. In particular:

- Do the merger simulations adequately describe the observed properties of ULIRGs?
- Do the properties of the stellar populations in ULIRGs correlate with other properties of ULIRGs, such as infrared luminosity, interaction class or spectral classification?
- What is the nature of the links between ULIRGs and other types of object in the local universe, such as QSOs, radio galaxies and elliptical galaxies?

Given their importance for studying the evolution of galaxies via major gas-rich mergers, it is perhaps surprising that there have been relatively few studies of stellar populations in ULIRGs. Many previous studies have concentrated on studying the SEDs and mid-IR emission line spectra of ULIRGs, with an emphasis on determining the dominant heating source for the MFIR-emitting dust (e.g. Farrah et al., 2003). However, such studies are not capable of determining the detailed properties of the stellar populations and how they vary with spatial location in these complex systems. Therefore, order to address the key issues

<sup>1</sup> The quantities  $f_{25}$  and  $f_{60}$  represent the *IRAS* flux densities in Janskys at  $25\mu\text{m}$  and  $60\mu\text{m}$ .

surrounding the evolution of ULIRGs we have undertaken a programme of deep optical long-slit spectroscopic observations of a substantial sample of nearby ULIRGs, aimed at investigating their star formation histories. In Rodríguez Zaurín et al. (2009a), hereafter Paper I, we presented the sample, data reduction and spectral synthesis modelling techniques. In this paper we discuss the results presented in Paper I in the context of evolutionary models for merging systems and the results obtained in studies of stellar populations in high- $z$  star forming galaxies.

Throughout this paper, we assume a cosmology with  $H_0 = 71 \text{ km s}^{-1} \text{ Mpc}^{-1}$ ,  $\Omega_0 = 0.27$ ,  $\Omega_\Lambda = 0.73$ .

## 2 MODELLING THE STELLAR POPULATIONS: GENERAL RESULTS

In Paper I we presented the results of spectral synthesis modelling of the complete (CS) and the extended (ES) samples, including 26 and 36 ULIRGs respectively. The detailed properties of these samples are described in that paper. To summarize, in the first place, we observed a complete RA-limited and declination-limited sub-sample of the Kim & Sanders (1998) 1 Jy sample of ULIRGs, with RAs in the range  $12 < \text{RA} < 1:30 \text{ h}$ , declinations  $\delta > -23$  degrees, and redshifts  $z < 0.13$ . The redshift limit was chosen to ensure that the objects are sufficiently bright for spectroscopic study, and also to keep the size of the sample tractable for deep observations on 4m class telescopes. We will refer to this sample of 26 objects as the complete sample (CS, see Table 1 in Paper I for details of some of the properties of the ULIRGs in the CS). In addition, we also observed 10 objects outside the redshift range and/or the RA and Dec range of the CS. With the aim of including a larger number of warm objects (only 8 warm ULIRGs are included in the CS), 7 of these 10 ULIRGs have warm mid- to far-IR colours. The sample including the CS and these 10 additional objects will be referred to as the extended sample (ES). Thus, the ES comprises 36 objects: 21 cool ULIRGs, and 15 warm ULIRGs. Since the ES accounts better for the diversity within the ULIRG phenomenon, and our statistical analysis shows no significant differences between the properties of the stellar populations in the ES and CS, we concentrate on the ES sample for the study presented in this paper.

In order to perform a detailed study of the stellar populations in ULIRGs, a total of 133 apertures was extracted for the objects in the ES. The extraction apertures were selected from spatial cuts of the 2-D frames in the line-free continuum wavelength range 4400 – 4600 Å, based on the visible extended structures and the requirement that the apertures are large enough to have a sufficiently high S/N ratio for further analysis. To compare the stellar populations between the objects in our sample, apertures with a metrical scale of 5kpc centred on the main nuclei were extracted for all the objects in the extended sample (ES), including separate extractions for multiple nuclei in individual sources. A second set of apertures was then selected to sample the spatial features of those objects in the ES showing tails, bridges and other diffuse structures.

To perform the fits, we have used the CONFIT code (see Robinson et al. 2000 and RZ08 for details). The CON-

FIT approach consists of a direct fit of the overall continuum shape of the extracted spectra using on a minimum  $\chi^2$  technique (Tadhunter et al., 2005; Rodríguez Zaurín et al., 2007). CONFIT is based on a “simplest model” approach, i.e. we fit the minimum number of stellar components required to adequately model the data. Therefore, CONFIT allows for a maximum of two stellar components plus a power-law in some cases. Throughout this paper, we define *young stellar populations* (YSPs) as stellar components with ages  $t_{YSP} \leq 2 \text{ Gyr}$ , and *old stellar populations* (OSP) as components with ages  $t_{OSP} > 2 \text{ Gyr}$ . With the aim of better describing each combination, it is convenient to further sub-divide the YSPs into two groups: *very young stellar populations* (VYSP): stellar components with ages  $t_{VYSP} \leq 0.1 \text{ Gyr}$ ; *intermediate-age young stellar populations* (IYSP): stellar components with ages in the range of  $0.1 < t_{IYSP} \leq 2 \text{ Gyr}$ .

Given that the properties of the stellar populations were not known a priori, three modelling combinations were investigated. The results obtained for each of the combinations are described in detail in Paper I, and are summarized as follows.

- **Combination I.** As a first approach we used a two component model comprising a YSP ( $t_{YSP} \leq 2 \text{ Gyr}$ ) with varying reddening ( $0.0 \leq E(B-V) \leq 2.0$ , increasing in steps of 0.1), along with an unreddened OSP of age 12.5 Gyr. Accounting for an old component covers the case in which one or more of the merging galaxies is early-type or bulge-dominated galaxy. Using this combination we obtained adequate fits ( $\chi_{\text{red}}^2 \leq 1.0$ ) to the overall shape of the SED for all but one (IRAS 23060+0505, for which a power-law is required) of the extraction apertures modelled. However, Comb I fails to adequately fit the absorption detailed absorption – particularly the CaII K feature – for  $\sim 42\%$  (54) of the apertures modelled<sup>2</sup>.

- **Combination II.** This combination consists of three components: an OSP of age 12.5 Gyr and zero reddening, along with a YSP with variable reddening ( $0.0 \leq E(B-V) \leq 2.0$ , increasing in steps of 0.1), and a power-law with a spectral index in the range  $-15 < \alpha < 15$ . The power-law is included to represent either scattered or direct AGN continuum component (Tadhunter et al., 2002), or a highly reddened VYSP. Adequate fits ( $\chi^2 \leq 1.0$ ) to the overall SED shapes were found for all of the apertures of all objects using this combination. On the other hand, this combination fails to fit the detailed absorption features for 10% (13 apertures) of the apertures modelled. We find that the minimum percentage contribution of the OSP component is less than 10% (due to the uncertainties inherent in the modelling techniques percentage contributions  $< 10\%$  are considered negligible) for most of the apertures. This result suggests that an OSP component is not required to fit the optical spectra of the majority of the objects in the ES.

- **Combination III.** A drawback of Comb II is that, for those cases in which the power-law is likely to represent a VYSP component, it gives no information about the detailed properties (age and reddening) of such a component. In addition, for ULIRGs as a class, there is no reason, a priori, to

<sup>2</sup> As discussed in paper I, some of this discrepancy may be due to the effect of ISM absorption on the CaII K resonance line.

expect a major contribution to the optical emission from a 12.5 Gyr OSP. Such lack of an OSP is also suggested by the results of Combination II. Therefore, in order to explore the possibility of YSPs dominating the optical emission from the objects we decided to use a combination consisting of two YSP components: a IYSP with ages in the range 0.3 – 2.0 Gyr, with  $E(B - V)$  values of 0.0, 0.2 or 0.4, plus a VYSP with age in the range 1 – 100 Myr and reddenings ( $0.0 \leq E(B - V) \leq 2.0$ , increasing in steps of 0.1). Adequate fits to both the continuum and the detailed absorption features are obtained for all but 9 ( $\sim 7\%$ ) of the extraction apertures modelled. In the minority of the cases for which no adequate fits could be obtained using Comb III, either an OSP or a power-law component was required in addition to a YSP.

Significantly, for the majority of apertures we find that both the SEDs and the detailed absorption features can be adequately modelled with all three combinations, although in most cases Comb III provides the best overall fit. This demonstrates that it can be difficult to derive a unique model solution even with high-quality, wide spectral coverage optical spectra. Nonetheless, the fits provide the following general results.

- **Dominant young stellar populations.** YSPs dominate the optical light, while OSPs are relatively unimportant, in the overwhelming majority of apertures modelled. In terms of the nuclear apertures, the only exceptions are IRAS 13451+1232 5kpc, IRAS 1648NE 5kpc, IRAS 21208-0519 5kpcII, IRAS 23233+2817 5kpc and IRAS 23327+2913 5kpcII. Although there is some ambiguity in the cases of IRAS 13451+1232 5kpc, IRAS 1648NE 5kpc, and IRAS 23233+2817 5kpc which can be modelled either in terms of a dominant OSP plus a YSP (Comb I) or a dominant “old” IYSP ( $>1$  Gyr) plus a VYSP (Comb III), we can only adequately model IRAS 21208-0519 5kpcII and IRAS 23327+2913 5kpcII with Comb I models that include an OSP. Note that, in the case of IRAS 23327+2913 5kpcII, it is possible to model the optical spectrum using an OSP, without any requirement for a YSP. Apart from these exceptions, for most objects the results are consistent with the idea that the precursor galaxies are gas-rich spiral galaxies.

- **Complex star formation histories.** Consistent with our previous results for the nearby ULIRG Arp220 (Rodríguez Zaurín et al., 2008), we find that most apertures of most objects are best fitted with models that include a combination of VYSP and IYSP (i.e. Comb III). This suggests that the recent star formation histories of most ULIRGs are complex, with at least two star formation epochs, even if the most recent (represented by the VYSPs) often dominates the optical light.

In the following sections we consider the properties of the YSP in ULIRGs in more quantitative detail, and investigate whether they are correlated with other properties of these merging systems.

## 2.1 Characteristic properties of the YSPs in the nuclear and extended regions.

As described in Paper I, Comb I (YSP + OSP) provides useful estimates of the “luminosity weighted” ages, reddenings

|        |                | Mean | Median |
|--------|----------------|------|--------|
| NUC AP | LW-age (Myr)   | 66   | 60     |
|        | LW- $E(B - V)$ | 0.4  | 0.4    |
|        | LW-%           | 77   | 82     |
| EXT AP | LW-age (Myr)   | 203  | 80     |
|        | LW- $E(B - V)$ | 0.2  | 0.2    |
|        | LW-%           | 63   | 66     |

**Table 1.** Mean and median values for the parameters associated with the YSPs for both the nuclear and extended regions of the objects in the ES, obtained using Comb I.

|                | D     | Confidence Level |
|----------------|-------|------------------|
| LW-age         | 0.325 | 99%              |
| LW- $E(B - V)$ | 0.50  | $> 99.9\%$       |
| LW-%           | 0.383 | $> 99.9\%$       |

**Table 2.** Results of the K-S test for the significance of differences between the distributions in the nuclear and the extended regions, of the LW-age, LW- $E(B - V)$  and LW-% for the ES and using Comb I. Col (2): the maximum deviation between the two cumulative distribution functions. Col (3): the probability that the difference between the distribution of the nuclear and the extended regions is significant.

and percentage contributions of the dominant YSPs within each galaxy. Providing a single estimate (with an associated uncertainty) for the parameters associated with the YSPs in each aperture, this combination is particularly useful for performing a statistical analysis of the properties of the stellar populations in the CS and the ES samples.

Figure 1 shows the distributions of the average luminosity-weighted ages (LW-age), reddenings (LW- $E(B - V)$ ) and percentage contributions to the flux in the normalising bin (LW-%) of the YSPs in the nuclear and extended apertures. This figure has been made using 34 of the 36 objects in the ES. For two of the three objects classified as Sy1 (IRAS 15462-0450 and IRAS 21219-1757) no extended apertures were extracted and, therefore, they are not included in the analysis presented here. In the case that one of the extended apertures samples a similar region to the 5 kpc aperture, only the latter is used for the plots (for example, ApE and 5 kpc in the case of Mrk 273). In the case of Arp 220, only two of the 24 apertures were included, in order to avoid giving too much weight to the extended apertures in a single object. These are the 5 kpc aperture and AP<sub>TOTAL</sub> for PA 75\*. Overall, a total of 100 of the 128 apertures modelled for the ES were eventually used for the figures.

The upper panel of Figure 1 shows the presence of a clear upper limit of 100 Myr for the LW-ages of the YSPs in the nuclear apertures; only  $\sim 9\%$  of the nuclear apertures (4 of the 44 nuclear apertures used) have average LW-ages older than this value. In contrast,  $\sim 41\%$  of the extended apertures (23 of the 56 extended apertures used) have average LW-age values older than 100 Myr, and as old as 1.2 Gyr. In terms of reddening, Figure 1 (middle) suggests the presence of higher reddening (LW- $E(B - V)$ ) values in the nuclear regions of the galaxies compared with the extended regions. We also find that the YSPs represent the dominant contribution (LW-%  $\geq 50\%$ ) to the optical emission for all

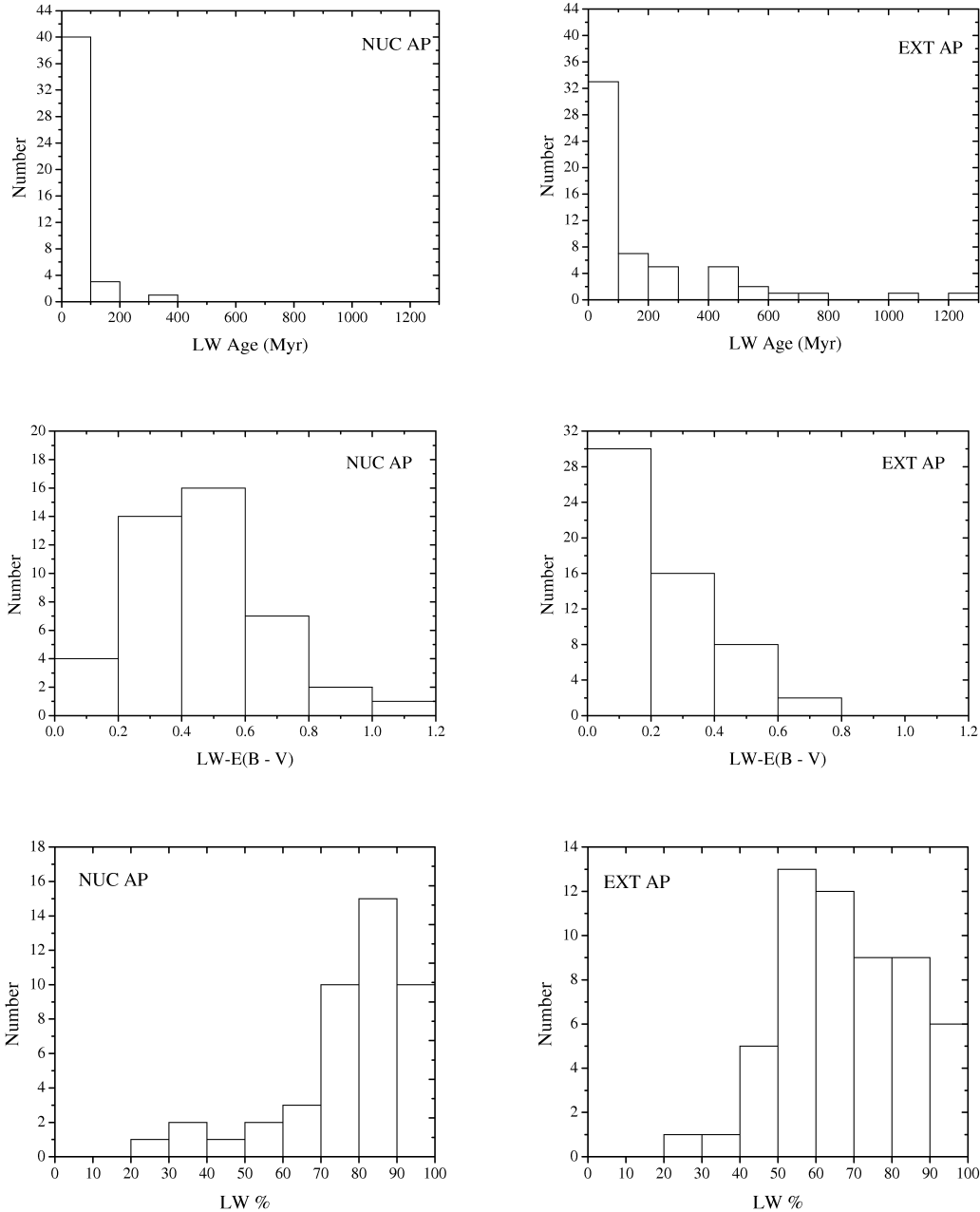


**Figure 1.** Histograms showing the LW-age (top), LW- $E(B - V)$  (middle), and LW-% (bottom) contribution distributions for the nuclear (left) 5 kpc and the extended (right) apertures. The results of Comb I show that YSPs are present at all locations in the galaxies for the majority of the objects in the ES, with a clear cut-off in YSP ages at 100 Myr in the case of the nuclear regions. The figure also suggests that the YSPs in the nuclear regions of the galaxies, coinciding with higher reddening, represent a more important contribution to the flux at optical wavelengths than those in the extended regions.

but 11 (11%) of the apertures used (4 nuclear apertures and 7 extended apertures, Figure 1; bottom panel). However, the YSP make a more important contribution to the optical light in the nuclear regions.

Table 1 shows the mean and median values of the different parameters associated with the YSPs. To investigate whether the distributions of the YSPs properties in the nuclear and extended regions are indeed different, we used the Kolmogorov-Smirnov (K-S) two sample test, and the results

are presented in Table 2. We find that the differences between the LW-age, LW- $E(B - V)$  and LW-% distributions for the YSPs in the nuclear and extended regions of the galaxies are significant with a confidence level of  $\gtrsim 99\%$  (i.e. the probability that the distributions are drawn at random from the same parent distribution is  $< 1\%$ ).

To further investigate the properties of the stellar populations, we performed a similar study to that presented above using the results of Comb III (VYSP + IYSP). Fig-

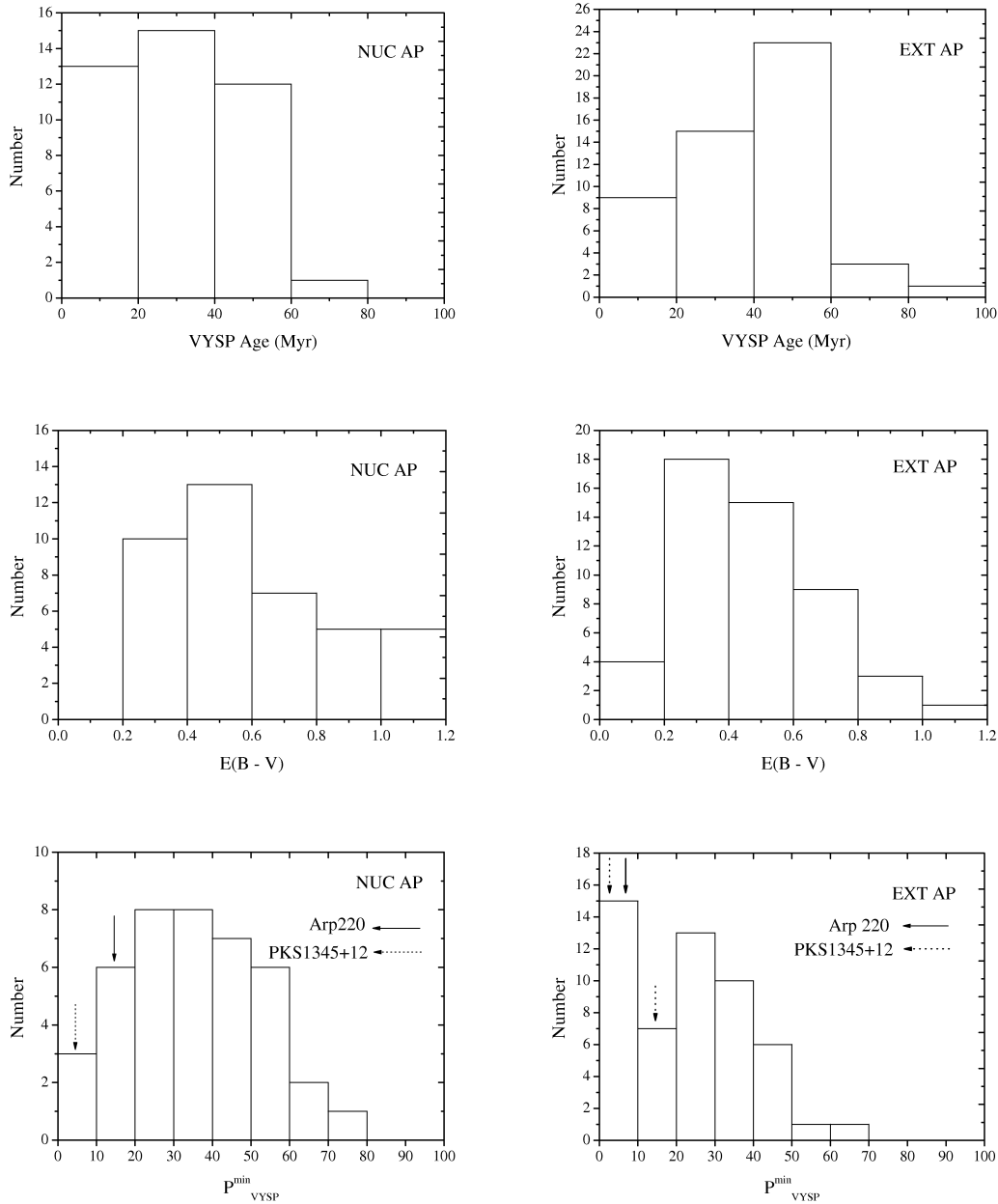


**Figure 2.** Histograms showing the distributions of the average VYSP-Age (top),  $E(B - V)$  values (middle) and the minimum percentage contribution to the flux in the normalising bin ( $P_{\text{VYSP}}^{\text{min}}$ , bottom) for the nuclear 5 kpc (left) and the extended (right) apertures, using the ES and Comb III. The locations of Arp 220 and PKS1345+12 are also shown in the figure.

|        |                                | Mean | Median |
|--------|--------------------------------|------|--------|
| NUC AP | VYSP-Age (Myr)                 | 31   | 30     |
|        | VYSP-E(B - V)                  | 0.6  | 0.6    |
|        | $P_{\text{VYSP}}^{\text{min}}$ | 37   | 39     |
| EXT AP | VYSP-Age (Myr)                 | 39   | 50     |
|        | VYSP-E(B - V)                  | 0.4  | 0.4    |
|        | $P_{\text{VYSP}}^{\text{min}}$ | 24   | 25     |

**Table 3.** Mean and median values for the parameters associated with the VYSPs, for both the nuclear and extended regions of the objects in the ES, obtained using Comb III.

ure 2 shows the distributions of the average values for the VYSPs age, reddening and the minimum percentage contribution to the flux in the normalising bin ( $P_{\text{VYSP}}^{\text{min}}$ ), for both the nuclear and the extended regions. From a visual inspection of the histograms, the modelling results suggest the presence of “younger” and more reddened VYSPs in the nuclear regions of the objects. Moreover, the lower panel in Figure 2 is designed to show the importance of the VYSPs within the different regions of the galaxies sampled by the apertures. The figure suggests that VYSPs are more important in the nuclear regions of the galaxies. Table 3 presents the mean and median values for the VYSP-Age, VYSP-E(B

|                                | D    | Confidence Level |
|--------------------------------|------|------------------|
| VYSP-Age (Myr)                 | 0.27 | 95%              |
| VYSP-E(B - V)                  | 0.27 | 95%              |
| $P_{\text{VYSP}}^{\text{min}}$ | 0.35 | 99.5%            |

**Table 4.** Results of the K-S test for the significance of differences between the distributions in the nuclear and the extended regions, of the VYSP-Age, VYSP-E(B - V) and  $P_{\text{VYSP}}^{\text{min}}$  for the ES, using Comb III. Col (1): the maximum deviation between the cumulative distribution functions Col (2): the probability that the difference between the distribution of the nuclear and the extended regions is significant.

- V) and  $P_{\text{VYSP}}^{\text{min}}$ , while Table 4 shows the results of the K-S test obtained using Comb III. We find that the difference between the VYSPs age and E(B - V) distributions in the nuclear and the extended regions is significant with a confidence level of 95%. In the case of  $P_{\text{VYSP}}^{\text{min}}$ , the confidence level is 99.5%. Overall, the results are consistent with those of Comb I, but the level of significance is lower.

The lower panel of Figures 2 also shows the locations of IRAS 13451+1232 (PKS1345+12) and Arp 220, the two objects for which detailed studies were presented in Rodríguez Zaurín et al. (2007) and Rodríguez Zaurín et al. (2008). Arp 220 is frequently used as the archetype of ULIRGs as a class. However, the modelling results indicate that the YSPs in this object are not typical of the objects ULIRGs in general. While significant VYSPs are detected at all locations of the galaxies sampled by the apertures, in the case of Arp 220 the contribution of such populations is relatively small, apart from in the nuclear region of the galaxy. Furthermore, in this object, a uniform IYSP of age 0.5 – 0.9 Gyr is found at all locations sampled by the apertures.

In the case of PKS 1345+12, some peculiarities might be expected, since this is the only object in our sample classified as radio galaxy. For this object, either OSPs or dominant “old” IYSPs (1 - 2 Gyr) are required to model the data (see Paper I for details); the contribution from VYSPs is relatively small. Independent of the combination of stellar populations assumed, this galaxy is the most massive amongst the objects in our sample (see Table 4 in Paper I).

Overall, our modelling results indicate that the VYSPs in the nuclear regions of the galaxies make a more significant contribution to the optical light than those of the extended regions. In terms of age and reddening, the VYSPs located in the nuclear regions tend to be younger and more reddened, although further analysis is required to confirm these results. This results will be discussed in the context of the merger simulations in Section 6.

## 2.2 Correlations between the properties of the YSP and other ULIRG properties

Given that certain of the general properties of ULIRGs (e.g. IR luminosities, mid- to far-IR colours, optical morphology and spectral class) may change as the systems evolve along the merger sequence, it is interesting to determine whether such properties correlate with those of the YSP determined from spectral synthesis modelling.

With the aim of investigating whether the more lu-

|       |                                | Mean | Median |
|-------|--------------------------------|------|--------|
| HII   | VYSP-Age (Myr)                 | 20   | 25     |
|       | VYSP-E(B - V)                  | 0.5  | 0.4    |
|       | $P_{\text{VYSP}}^{\text{min}}$ | 46   | 40     |
| LINER | VYSP-Age (Myr)                 | 35   | 35     |
|       | VYSP-E(B - V)                  | 0.6  | 0.6    |
|       | $P_{\text{VYSP}}^{\text{min}}$ | 34   | 34     |
| Sy2   | VYSP-Age (Myr)                 | 28   | 25     |
|       | VYSP-E(B - V)                  | 0.6  | 0.6    |
|       | $P_{\text{VYSP}}^{\text{min}}$ | 43   | 50     |

**Table 5.** Mean and median values of the VYSP-Age, VYSP-E(B - V) and  $P_{\text{VYSP}}^{\text{min}}$  for the HII, LINER and Sy2-ULIRGs, for the nuclear 5 kpc apertures.

minous objects have younger, redder or more important VYSPs, Figure 3 shows the average VYSP age, reddening (E(B - V)) and minimum percentage contribution ( $P_{\text{VYSP}}^{\text{min}}$ ) obtained for the nuclear 5 kpc apertures, plotted against the log of the IR-luminosity (from Kim & Sanders 1998). Note that, since it was not possible to model the Sy1-ULIRGs (IRAS 12540+5708, IRAS 15462-0450 and IRAS 21219-1757, see Paper I for details), no Sy1 galaxies are shown in the figure. We find that the properties of the VYSPs are independent of the IR-luminosities of the sources.

In addition to looking for trends with luminosity we can also examine whether the stellar properties depend on the optical spectral classification. As can be seen from Figure 3, where the points are labelled according to spectral classification, we see no clear trend with optical type. Table 5 shows the mean and median values of the VYSP age, reddening and  $P_{\text{VYSP}}^{\text{min}}$  for the different types of object i.e. HII-, LINER- and Sy2-ULIRGs. If, for example, there exists an evolutionary link between the HII- or LINER-ULIRGs and the Sy2-ULIRGs (Sanders et al, 1988b), the latter representing a more advanced stage in an evolutionary sequence, one might expect the Sy2-ULIRGs to have older ages. No trends are observed in Figure 3 for the different types of ULIRGs. A first interpretation is that there is no evolutionary link between HII-, LINER- and Sy2-ULIRGs. However, it is also possible that the transition between one type and the other occurs over a shorter timescale than the typical timescale of the enhancement of the star formation activity in the final stages of the merger event as the nuclei coalesce ( $\sim 100$  Myr, Barnes & Hernquist, 1996). In that case, no trend is expected to be observed.

We have also investigated the presence of correlations between the properties of the VYSPs and other properties of ULIRGs such as the Veilleux et al. (2002) interaction class, or the MFIR colour ratio  $f_{25}/f_{60}^3$ . The conclusions reached are identical, i.e. no evidence for correlations or trends is found.

As well as the explanation already discussed above, possible reasons for the lack of correlations between the YSP properties and other properties of ULIRGs include the following:

<sup>3</sup> The quantities  $f_{25}$  and  $f_{60}$  represent the IRAS flux densities in Jy at  $25\mu\text{m}$  and  $60\mu\text{m}$ .

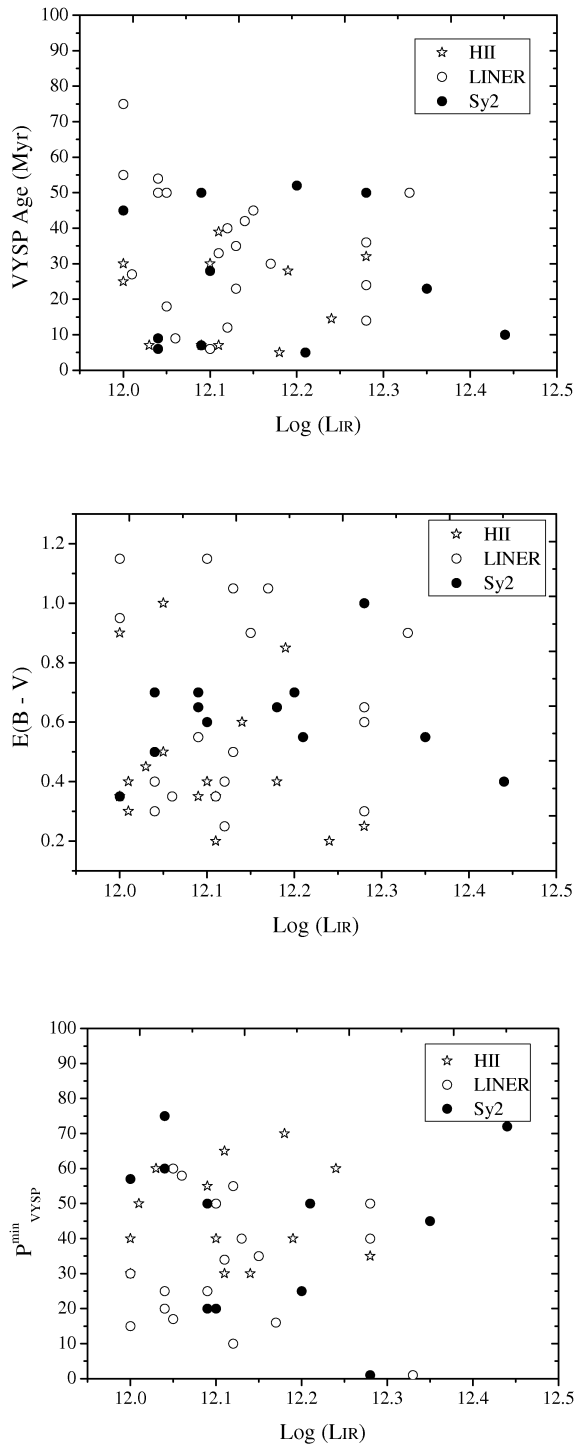


**Figure 3.** Average VYSP age,  $E(B - V)$ , and  $P_{\text{VYSP}}^{\text{min}}$  plotted against  $\text{Log}(L_{\text{IR}})$ . The nuclear 5 kpc apertures have been used for these plots. The points are labelled based on the Veilleux et al. (1999) spectral classifications. No significant correlations are observed.

- **Modelling technique:** the outputs of the modelling technique used for the analysis presented in this section, as described in detail in Paper I, are ranges of age, reddening and percentage contribution of both IYSPs and VYSPs. Therefore, part of the scatter in the YSP properties could be due to the uncertainties inherent in the modelling technique; such uncertainties could hide underlying trends and patterns in behaviour.

- **Other variables:** there are other variables such as, for example, the gas contents of the parent galaxies or the geometry of the merger, that could have a more important impact on the properties of the VYSPs in ULIRGs than the spectral classification, MFIR colours, MFIR luminosities, or the interaction class.

Interestingly, this apparent lack of correlations between the various properties of ULIRGs has been found by other authors. Veilleux et al. (1999) found no correlation between the emission line reddenings and other properties of ULIRGs, such as the MFIR colour ratio  $f_{25}/f_{60}$ , for the 108 objects in their sample. Moreover, Farrah et al. (2001) carried out an *HST*-WFPC2 V-band imaging study of a sample of 23 ULIRGs and found no correlation between the IR-luminosity and the morphologies of the objects in their sample.

### 3 THE MASSES OF THE YSPS

Table 4 in Paper I presents estimates for the total stellar masses associated with the different stellar components for the objects in the ES. Figure 4 shows the distribution of the total stellar masses presented in that table (accounting for all VYSP, IYSP and OSP if present). Note that, in the cases of IRAS 14394+5332, IRAS 17028+5817 and IRAS 23327+2913, the total stellar mass was estimated for the two nuclei individually and, for the purpose of the figure, the masses of the two nuclei were added. The figure shows that only 6 objects in our sample — IRAS 00188-0856, IRAS 13451+132, IRAS 14348-1447, IRAS 17179+5444, IRAS 23233+2819 and IRAS 23327+2913 — have stellar masses  $M_{\text{stellar}} > 1 \times 10^{11} M_{\odot}$ . Although two of these objects — IRAS 1345+132, IRAS 17179+5444 — are spectroscopically classified as Sy2 galaxies in the optical, overall there is no clear-cut distinction between Seyfert and non-Seyfert ULIRGs in terms of their stellar mass; many Seyfert ULIRGs have stellar masses that are relatively modest — at or below the median for the sample as a whole. Thus our results provide no clear support for the idea that AGN activity in ULIRGs is more likely to be associated with relatively early-type galaxies with massive bulges, as appears to be the case in large samples of galaxies drawn from the Sloan Digital Sky Survey (SDSS) (Kauffmann et al., 2004; Heckman et al., 2004).

In order to compare the results found here with other studies, Table 6 shows the total mass values in units of  $m_*$ , defined as the break in the measured mass function obtained from a large sample of 17,173 galaxies drawn from a combination of the Two Micron All Sky survey (2MASS) Extended Source catalogue and the 2dF galaxy redshift survey ( $m_* = 1.4 \times 10^{11} M_{\odot}$ ; Cole et al., 2001, adapted to our cosmology). For the ES sample as a whole, the stellar masses are in the range  $0.1 m_* \leq M_{\text{stellar}} \leq 3.6 m_*$ , with a



| Object Name<br>IRAS | $M_{\text{stellar}}$<br>( $m_*$ ) | $M_{\text{dyn}}^1$<br>( $m_*$ ) | $M_{\text{dyn}}^2$<br>( $m_*$ ) | $M_{\text{dyn}}^3$<br>( $m_*$ ) |
|---------------------|-----------------------------------|---------------------------------|---------------------------------|---------------------------------|
| 00091-0738          | 0.33                              | ...                             | ...                             | ...                             |
| 00188-0856          | 0.72                              | ...                             | ...                             | ...                             |
| 01004-2237          | 0.11                              | ...                             | ...                             | 0.07                            |
| 08572+3915          | 0.20                              | ...                             | 0.13                            | ...                             |
| 10190+1322          | 0.28                              | ...                             | ...                             | 0.93                            |
| 10494+4424          | 0.37                              | ...                             | ...                             | ...                             |
| 12072-0444          | 0.26                              | ...                             | ...                             | ...                             |
| 12112+0305          | 0.52                              | ...                             | 0.70                            | 0.40                            |
| 12540+5708          | ...                               | ...                             | ...                             | ...                             |
| 13305-1739          | 0.28                              | ...                             | ...                             | ...                             |
| 13428+5608          | 0.53                              | 2.0                             | 0.6 - 1.1                       | 0.88                            |
| 13451+1232          | 3.60                              | ...                             | ...                             | ...                             |
| 13539+2920          | 0.24                              | ...                             | ...                             | ...                             |
| 14060+2919          | 0.40                              | ...                             | ...                             | ...                             |
| 14252-1550          | 0.38                              | ...                             | ...                             | ...                             |
| 14348-1447          | 0.77                              | 1.0                             | 1.1                             | 1.50                            |
| 14394+5332          | 0.44                              | ...                             | ...                             | ...                             |
| 15130-1958          | 0.28                              | ...                             | ...                             | 0.51                            |
| 15206+3342          | 0.60                              | ...                             | 0.3                             | ...                             |
| 15327+2340          | 0.25                              | 0.3                             | 0.3                             | 0.26                            |
| 16156+0146          | 0.22                              | ...                             | ...                             | ...                             |
| 16474+3430          | 0.61                              | ...                             | ...                             | ...                             |
| 16487+5447          | 0.67                              | ...                             | ...                             | ...                             |
| 17028+5817          | 0.40                              | ...                             | ...                             | ...                             |
| 17044+6720          | 0.19                              | ...                             | ...                             | ...                             |
| 17179+5444          | 1.24                              | ...                             | ...                             | ...                             |
| 20414-1651          | 0.25                              | ...                             | ...                             | 0.52                            |
| 21208-0519          | 0.68                              | ...                             | ...                             | ...                             |
| 22491-1808          | 0.20                              | ...                             | ...                             | 0.68                            |
| 23060+0505          | 0.49                              | ...                             | ...                             | ...                             |
| 23233+2817          | 1.64                              | ...                             | ...                             | ...                             |
| 23234+0946          | 0.34                              | ...                             | ...                             | ...                             |
| 23327+2913          | 3.37                              | ...                             | ...                             | ...                             |
| 23389+0303          | 0.15                              | ...                             | ...                             | ...                             |

**Table 6.** Estimated total masses associated with the stellar populations (YSPs, including VYSPs and IYSPs, and OSPs if present) detected at optical wavelengths, expressed in units of  $m_*$  ( $m_* = 1.4 \times 10^{11} M_{\odot}$ ). Due to the powerful AGN emission, it was not possible to estimate the total mass for the three objects in our sample classified as Sy1 galaxies (IRAS 12540-5708, IRAS 15462-0405 and IRAS 21219-1757).

<sup>1</sup> Dynamical mass from Tacconi et al. (2002).

<sup>2</sup> Dynamical mass from Colina et al. (2005).

<sup>3</sup> Dynamical mass from Dasyra et al. (2006a,b).

mean value of  $0.6 m_*$  and a median of  $0.4 m_*$ . Approximately 80% of the objects in the ES (27) have total stellar masses  $M_{\text{stellar}} < 1 \times 10^{11} M_{\odot}$  ( $0.71 m_*$ ). Also shown in the table are the dynamical mass estimates (including stars, gas and dark matter) from Tacconi et al. (2002), Colina et al. (2005) and Dasyra et al. (2006a,b) for the objects in common with the ES. The values presented in the table are for the entire systems, including the extended regions of the galaxies and adding the dynamical masses of the two nuclei for the double nucleus systems. To measure the dynamical mass of the systems, Tacconi et al. (2002) and Dasyra et al. (2006a,b) used near-IR CO and Si I absorption features, tracing the stars in the galaxies, although Dasyra et al. (2006a,b) also used the [Fe II] forbidden emission line, which is a tracer of the warm, ionized gas. In contrast, Colina et al. (2005) used the optical H $\alpha$  emission line, which also traces the warm, ionized gas. The main uncertainties associated with these techniques are: (1) the internal extinction; (2) the light contribution from AGN and/or compact, nuclear starburst; and

(3) the assumption of virialization (for a detailed discussion see Colina et al., 2005). A comparison between our modelling results and those of the kinematical studies mentioned above shows that:

- typically the stellar masses are within a factor of  $\sim 2$  of the dynamical masses, which is remarkable given the uncertainties in both spectroscopic and dynamical techniques;
- the dynamical masses tend to be larger than the stellar masses in most cases. However this is not surprising given that the dynamical masses account for all the mass (including stars, gas and dark matter), whereas the spectroscopic masses only account for the stars.

The results presented here reinforce the idea that ULIRGs are sub- $m_*$  or  $\sim m_*$  systems (Genzel et al., 2001; Tacconi et al., 2002; Colina et al., 2005; Dasyra et al., 2006a,b). They also provide evidence that the optically visible stellar populations dominate the stellar masses of the

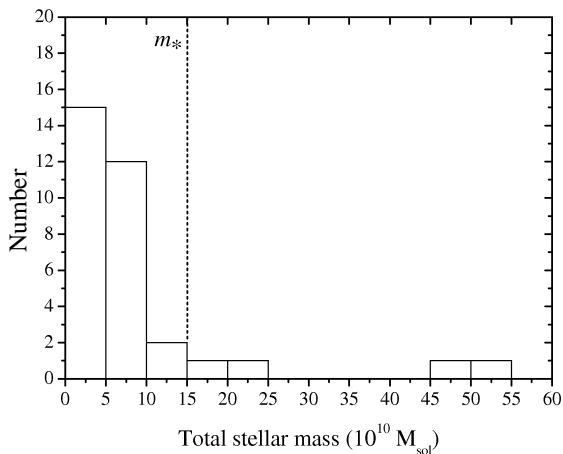


**Figure 4.** Histogram showing the distribution of the total stellar mass values presented in Table 6 for the objects in the ES. The figure shows that only 6 of the objects have stellar masses  $M_{\text{stellar}} > 1 \times 10^{11} M_{\odot}$ .

systems; the mass contributions of any stellar populations entirely hidden by dust must be relatively minor.

#### 4 BOLOMETRIC LUMINOSITIES: HIDDEN STARBURST COMPONENTS

As well as the total stellar masses, the estimated values for the bolometric luminosities associated with the stellar populations detected at optical wavelengths are also presented in Table 4, of Paper I. For the ES, we find a mean value of  $L_{\text{bol}} = 0.66 \times 10^{12} L_{\odot}$  and a median of  $L_{\text{bol}} = 0.53 \times 10^{12} L_{\odot}$ . Assuming that most of the optical light is absorbed and re-processed by dust, it is possible to compare these values with the mid- to far-IR luminosities of the sources. Figure 5 presents a histogram showing the estimated bolometric luminosities of the YSPs detected in the optical expressed as percentages of the mid- to far-IR luminosities of the 33 sources in the ES considered here (all but the three Sy1, for which it was not possible to estimate  $L_{\text{bol}}$ ). We find that for 48% of the objects (16 of 33) the bolometric luminosities of the YSPs detected at optical wavelengths represent a large fraction ( $\gtrsim 50\%$ ) of the mid- to far-IR luminosities of the sources.

However, note that 6 of the 16 objects in which  $L_{\text{bol}}(\text{YSP})$  represents a large fraction of the  $L_{\text{IR}}$  are spectroscopically classified as Sy2 galaxies in the optical. Due to potential AGN contamination, the contribution of the stellar populations to the optical light, and therefore the bolometric luminosity associated with them, is less well constrained for these objects than for the other ULIRGs. Hence, it is possible that the true values of the stellar bolometric luminosity presented in Paper I are significantly smaller. Excluding these 6 objects from the group of 16, we find that in 23 of the remaining 33 objects in the ES (70%) the bolometric luminosities of the YSPs represent only a modest fraction of mid- to far-IR luminosities ( $L_{\text{YSP}}/L_{\text{IR}} < 0.5$ ). On the other hand, there remain 10 objects in the ES ( $\sim 30\%$ ), with no

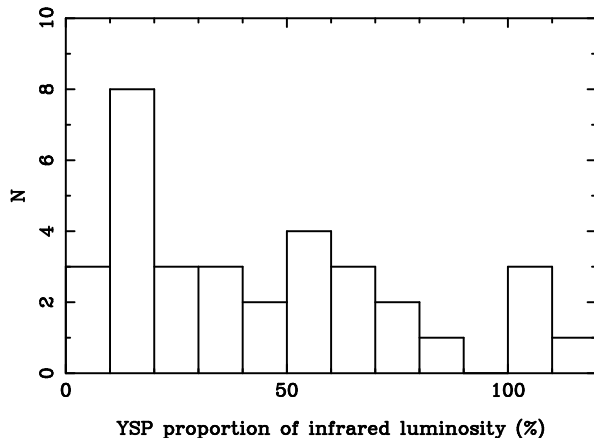


**Figure 5.** Histogram showing the estimated bolometric luminosities of the YSPs detected in the optical expressed as percentages of the mid- to far-IR luminosities of the 33 sources in the ES considered here.

evidence of AGN activity, for which we find that the YSP luminosities represent a large proportion of their infrared luminosities.

At this stage, it is important to mention that there are two major uncertainties associated to the results presented in this section: first, uncertainties in the selection of a particular model that is then applied to the whole galaxy; second, the assumption that all the stellar light is actually absorbed by, and heats the dust that radiates at mid- to far-IR wavelengths. In the former case, our model selection and assumptions are unlikely to be substantially in error, since the stellar masses derived from the same models compare well with the dynamical masses. Of more concern is the second assumption: that all the light from the stellar populations heats the dust. In at least some cases, the reddening of the YSP in the nuclear aperture is fairly modest (see paper I for details) and the IYSP reddening is constrained to be  $E(B-V)$  of 0.4 or less. In the extended regions not covered by the slit (but included in our bolometric luminosity estimates because of the aperture correction of the flux), the reddening is likely to be even less. Therefore it is possible that a substantial fraction of the starlight from the stellar populations detected in the optical escapes each galaxy, and that the stellar bolometric luminosities presented in Table 10 in paper I and Figure 5 in this paper represent over-estimates of the ability of the starlight to heat the dust.

#### 5 THE NATURE OF THE PROGENITOR GALAXIES

We discuss in this section the extent to which the stellar populations detected in the optical have been formed during the merger, and also the nature of the progenitor galaxies involved in the triggering events. The aim is to answer two simple, but important, questions. First, are the YSPs detected in optical observations of ULIRGs all formed during the merger event? Second, can we use studies similar to that presented here in order to determine the star formation histories in major galaxy mergers?

As outlined Rodríguez Zaurín et al. (2008), the contamination by YSPs present in the disks of the galaxies prior to

the merger is potentially an important issue. We investigate this by comparing the VYSPs masses of late-type spirals, likely progenitors of ULIRGs, with those of the IYSPs in the ULIRGs in our ES. The reason to focus on the VYSPs in spirals is that, if the star formation is truncated during the merger, these are the stellar populations that may evolve into the IYSPs observed today. For the ULIRGs in the ES, we obtain IYSP masses in the range  $M_{\text{IYSP}} = 0.5 - 50 \times 10^{10} M_{\odot}$ , with a mean value of  $6.0 \times 10^{10} M_{\odot}$  and a median of  $3.4 \times 10^{10} M_{\odot}$  (see paper I)<sup>4</sup>. In comparison, Rodríguez Zaurín et al. (2008) estimated that the VYSP of typical late-type (Sc) spiral galaxies have VYSP masses in the range  $M_{\text{VYSP(Sc)}} = 1.2 - 8.5 \times 10^9 M_{\odot}$ . Therefore it is clear that, assuming an equal mass merger, both of the progenitor spiral galaxies must be at the upper end of the mass range in order to explain the IYSPs in ULIRGs in terms of VYSP from the captured disks of the progenitor galaxies; clearly the ULIRGs with the more massive IYSPs would be difficult to explain in this way.

Alternatively, we can consider the nature of the progenitor galaxies that would be required to produce the YSP (IYSP and VYSP) and gas masses of ULIRGs by gas-rich mergers, with the YSP formed entirely by merger-induced star formation. The total gas masses  $M(\text{H}_2 + \text{HI})$  of ULIRGs are typically of order a few times  $10^{10} M_{\odot}$  (Mirabel & Sanders, 1988; Solomon et al., 1997; Evans et al., 2002). Adding these gas masses to the total masses of the IYSP and VYSP (from Table 4 in paper I) that we are assuming have formed in the mergers, we find a total mass  $M(\text{gas} + \text{YSP}) > 5 \times 10^{10} M_{\odot}$  in many of the objects in our sample. Given that the merger-induced star formation is unlikely to be more than 50% efficient, the progenitor galaxies are together required to have an even larger gas mass. In comparison, typical late type (Sc) spiral galaxies have total gas masses of  $M(\text{H}_2 + \text{HI}) \sim 1.4 \times 10^{10} M_{\odot}$  (see Rodríguez Zaurín et al., 2008, for details). Therefore the progenitor galaxies are required to be at the upper end of the mass range for late-type spirals to explain the total YSP and gas masses of the ULIRGs. Note that, even if we consider only the gas masses, we require two “average” late-type spiral galaxies to merge in order to produce the typical gas masses measured in ULIRGs, and this is without accounting for any losses of gas due to outflows and star formation in the merger.

Finally we note that 33% of the objects in the ES have VYSPs with masses  $M_{\text{VYSP}} \gtrsim 10^{10} M_{\odot}$  (see paper I). Since these VYSP must be formed during the merger, and the star formation efficiency is likely to be  $< 50\%$ , the total amount of gas required in the progenitor galaxies is much larger; again a merger of two late-type spirals of average or larger mass would be required to produce the VYSP alone in these systems.

Overall, regardless of whether the IYSP are formed during the mergers or merely captured from the progenitor disks, it is clear that the progenitor galaxies are required to be massive gas-rich spiral galaxies. Using the compilation of HI masses in Roberts & Haynes (1994), we find that, for

the cases in which the estimated total progenitor gas mass is  $M(\text{gas} + \text{YSP}) > 5 \times 10^{10} M_{\odot}$ , both progenitor galaxies are required to be in upper 25% of the gas mass range for spirals<sup>5</sup>.

At this stage, it is important to add a caveat about the nature of the progenitor galaxies. It is commonly accepted that the ULIRG phenomenon is associated with gas-rich mergers in which both galaxies are spiral galaxies. This is supported by the mass arguments presented above, as well as the lack of evidence for a major contribution from an OSP in most of the ULIRG sample. However, in the cases of one of the nuclear apertures in each of the double nucleus systems IRAS 21208-0519 and IRAS 23327+2913, adequate fits are only obtained with a combination of stellar populations that includes a dominant contribution of a 12.5 Gyr OSP, plus a VYSP. Overall, these results suggest that mergers in which at least one of the progenitors had an early-type morphology can also trigger the ULIRG phenomenon.

## 6 COMPARISON WITH MERGER MODELS

The range of different morphologies of the objects in the ES, from widely separated double nuclei systems (e.g. IRAS 14394+5332) to single nucleus galaxies with no strong signs of tidal structures (e.g. IRAS 15206-3342), suggests that they are in different stages of merger events. In this section, we give an overview of how our modelling results fit in with the merger simulation predictions.

In general terms, the simulations predict two epochs of starburst activity (Mihos & Hernquist, 1996; Barnes & Hernquist, 1996; Springel et al., 2005) in major gas-rich mergers: the first occurring around or just after the first encounter, and a second more intense episode towards the end of the merger,  $\sim 0.5 - 1.5$  Gyr after the first encounter, when the nuclei are close to coalescing (within  $5 \times 10^7$  Myr of coalescence). However, both the time lag and the relative intensity of the peaks of starburst activity during the merger event depend on several factors: the presence of bulges, feedback effects, gas content and orbital geometry. For example, the presence of a bulge acts as a stabilizer of the gas against inflows and the formation of bar structures, allowing stronger starburst activity towards the end of the merger event (Mihos & Hernquist, 1996; Barnes & Hernquist, 1996). On the other hand, AGN feedback effects (e.g. quasar-driven winds) disrupt the gas surrounding the black hole, acting against the star formation activity at all stages (Springel et al., 2005).

In Paper I we showed that it is possible to model all of the extracted spectra with a combination of two stellar populations, plus a power-law in some cases. Concentrating again on comb III, the modelling results are, in general terms, consistent with the merger simulations. For example, it is possible that the IYSPs detected in most apertures are related to the first enhancement of the starburst activity, around or just after the time of the first encounter, and we are now seeing the objects at a later stage.

<sup>4</sup> It is important to emphasize that the upper limit of the range is found for the radio galaxy IRAS 13451+1232, which clearly represents an exceptional case among the ULIRGs in the ES

<sup>5</sup> Assuming an  $\text{H}_2/\text{HI}$  mass ratio of 0.7 for spirals (Young & Knezek, 1989).

We emphasize that, although the VYSPs are more significant in the nuclear regions of the galaxies, this component is detected at all locations sampled by the extended apertures for the overwhelming majority of the objects. We also find a trend for the VYSPs in the nuclear regions to be younger and more reddened than those of the extended regions. All of these results are consistent with the merger simulations, which predict that the star formation activity in the final stages of merger is concentrated towards the nuclear regions of the merging galaxies, coinciding with higher concentrations of gas and dust, but it also occurs within the tidal structures formed during the interaction. Furthermore, as described in Section 2, when using Comb I, we find a clear cut-off in YSP ages at 100 Myr in the nuclear regions. This is in good agreement with the timescale ( $\leq 100$  Myr) of the induced starburst activity predicted by the theoretical models for the final stages of a merger, as the nuclei coalesce (Mihos & Hernquist, 1996; Springel et al., 2005).

We note that ongoing star formation activity is also detected for all objects with relatively wide nuclear separations: IRAS 14394+5332<sup>6</sup> (54 kpc), IRAS 17028+5817 (25 kpc), IRAS 21208-0519 (15 kpc) and IRAS 23327+2913 (24 kpc). Three of these objects, IRAS 17028+5817, IRAS 21208-0519 and IRAS 23327+2913, show no signs of AGN activity. Star formation rates of  $\text{SFR} \gtrsim 100 M_{\odot} \text{ yr}^{-1}$  are required in order to produce the infrared luminosities ( $L_{\text{IR}} \geq 10^{12} L_{\odot}$ ) in these latter objects (Kennicutt, 1998). As noted above, such high star formation rates are only predicted by the merger simulations in two stages during the merger event:

- at, or after, the first encounter, if the parent galaxies have insignificant bulges and feedback effects are not important, or
- at the end of the merger event, close (within  $\sim 50$  Myr) to the coalescence of the nuclei.

Estimates of the dynamical timescales for completion of the mergers ranges from  $\geq 50$  Myr in the case of IRAS 21208-0519, to  $\geq 80$  Myr in the cases of IRAS 17028+5817 and IRAS 23327+2913<sup>7</sup>. Therefore, if the star formation activity is associated with the final starburst that occurs around the time of the coalescence of the nuclei, then this starburst must be relatively long-lived in these three wide separation systems. Alternatively, the enhanced star formation activity in these systems may be associated with the (relatively extended) period of star formation that follows as the galaxies move apart the first encounter of the two nuclei. However, for the latter case, the existing merger simulations do not predict the large star formation rates ( $\gtrsim 100 M_{\odot} \text{ yr}^{-1}$ ) for the extended period after the first encounter, that would be required for these systems to be observed as ULIRGs. Most probably, these wide nuclear separation ULIRGs are

systems in which the final starburst has been triggered relatively early in the period prior to coalescence, as the nuclei move together.

## 7 EVOLUTIONARY SCENARIOS

The presence of evolutionary links between ULIRGs, QSOs/radio galaxies and elliptical galaxies is commonly accepted. However, the true nature of the links remain uncertain. While some authors propose the evolutionary sequence cool ULIRG  $\rightarrow$  warm ULIRG  $\rightarrow$  optically selected QSO or radio galaxy (Sanders et al. (1988a); Canalizo & Stockton 2001), other authors (Genzel et al., 2001; Tacconi et al., 2002) dismiss such an evolutionary sequence based on the location of ULIRGs in the fundamental plane, similar to that of the intermediate mass ( $\sim L_{*}$ ) elliptical galaxies. We will compare here our study of a sample of 36 ULIRGs with studies of the stellar populations in samples of QSOs and related objects.

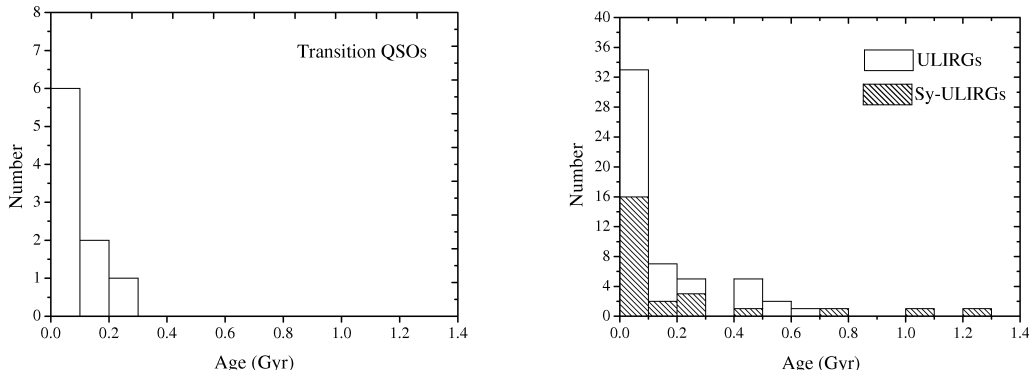
Canalizo & Stockton (2000a,b, 2001) carried out a similar study to that presented here for their sample of 9 “transition QSOs” — objects that may represent a transitional stage between ULIRGs and QSOs. All of their sample objects show clear signs of interaction, and five of them are classified as major mergers. Furthermore, all but one have infrared luminosities  $L_{\text{IR}} \geq 10^{12} L_{\odot}$  (i.e. they are ULIRGs). In order to study a possible link between these objects and the general populations of ULIRGs, Canalizo & Stockton investigated the stellar populations within the host galaxies. For that purpose, they modelled the optical spectra extracted from a series of extended apertures using a combination of a 10 Gyr OSP plus YSPs with varying ages, which is similar to the Comb I used here.

Figure 6 presents histograms comparing the distribution of the YSP ages derived by Canalizo & Stockton (2000a,b, 2001) for the transition QSOs, with those obtained for the ULIRGs in the ES sample using Comb I (labelled as LW-age in Section 3). For the transition QSOs, we have used the starburst peak ages (Canalizo & Stockton, 2001, column 5 of their Table 3), defined as the predominant starburst age found in the host galaxy (see Canalizo & Stockton, 1997, 2000a,b, for details), while for the ULIRGs we have used the average values of the LW-age, i.e. the same as in Figure 1. Note that, since the nuclear regions could not be sampled due to contamination by the bright quasar nuclei, the Canalizo & Stockton studies concentrate on the extended regions of the objects. Therefore, we have compared their results with those for the extended regions of the ULIRGs in the ES. Figure 6 also shows the results obtained in this study for the extended apertures of the Sy-ULIRGs (the “oldest” ages in this figure are obtained for the atypical object PKS1345+12).

As described in Section 2, we do not find any significant differences between the ages obtained for the HII- and LINER-ULIRGs and those of the Sy-ULIRGs in the ES. The same conclusions are reached if we compare the transition QSOs with the Sy-ULIRGs in the ES sample, or with the sample of ULIRGs as a whole. If there is an evolutionary link between ULIRGs as a class and the transition QSOs, one would expect the latter to have, in general, older YSP ages than ULIRGs, although some overlap is expected. How-

<sup>6</sup> Note that in the case of IRAS 14394+5332, the widest separation system in the sample, the ULIRG phenomenon is not related with the interaction of the two, widely separated systems, but with the eastern source, which is itself a merger in its final stages.

<sup>7</sup> In making these dynamical timescale estimates we have assumed that the projected distances between the nuclei represent their true separation, and that the nuclei are moving radially towards each other with a relative radial velocity of  $300 \text{ km s}^{-1}$ .



**Figure 6.** The young stellar age distribution for the Canalizo & Stockton (2001) transition QSOs (left) and the extended regions of the ULIRGs in the ES (right), with Seyfert ULIRGs highlighted. These results are based on modelling combination I. It is clear that the transition QSOs, Seyfert ULIRGs, and non-Seyfert ULIRGs overlap in terms of their distributions of YSP ages in these diagrams.

ever, it is clear from the figure that the ages obtained for the extended apertures in the transition QSOs are very similar to those of the extended apertures of the ULIRGs in the ES. A first interpretation of this result is that there is no clear evolutionary link between non-Seyfert ULIRGs and transition QSOs. However, as mentioned in section 2, it is possible that the timescale for the transition from ULIRGs to QSOs is smaller than the timescale associated with the ULIRG phenomenon.

Therefore, our study does not provide any clear-cut evidence for an evolutionary link between ULIRGs and the QSOs. Certainly, it is unlikely that the AGN in the Seyfert ULIRGs in our sample have been triggered a substantial period ( $> 100$  Myr) *after* the main merger-induced starburst, as appears to be the case in some radio galaxies (Tadhunter et al., 2005; Wills et al., 2008)

## 8 COMPARISON WITH STUDIES OF HIGH-Z OBJECTS

Star-forming galaxies have been detected in large numbers at high redshifts ( $z \gtrsim 1$ ). These galaxies are selected on the basis of their strong UV emission (Lyman-break galaxies – LBGs: see Giavalisco, 2002, for review), high sub-millimeter luminosities (sub-mm galaxies – SMGs, Smail et al., 2002; Blain et al., 2002; Chapman et al., 2003; Pope et al., 2005) mid-IR flux densities ( $24\mu\text{m}$  *Spitzer*-selected galaxies<sup>8</sup>, Papovich & et al., 2004; Caputi et al., 2006; Yan et al., 2007; Sajina et al., 2007; Farrah et al., 2008), or red near-IR colours:  $(J - K)_{\text{vega}} \gtrsim 2.3$  (distant red galaxies – DRGs, Franx et al., 2003). A large fraction show morphological features suggesting that major mergers are common among such objects (Giavalisco, 2002; Chapman et al., 2003; Erb et al., 2003, 2004; Conselice et al., 2005). In addition,

<sup>8</sup> Note that within the so called  $24\mu\text{m}$  *Spitzer*-selected galaxies class there will be galaxies classified as LBGs, SMGs and DRGs. However, not all LBGs and/or DRGs will be detected at  $24\mu\text{m}$  and therefore, we refer to the  $24\mu\text{m}$  *Spitzer*-selected objects as a class of galaxies with their own properties.

| Star forming galaxy type       | $M_{\text{stellar}} 10^{10} M_{\odot}$ | references             |
|--------------------------------|--|------------------------|
| Lyman-break                    | 0.2 - 6.0                              | Papovich et al. (2001) |
| Sub-mm                         | 12 - 25                                | Tacconi et al. (2008)  |
| Distant Red                    | 2.9 - 46.0                             | Papovich et al. (2006) |
| $24\mu\text{m}$ <i>Spitzer</i> | 0.1 - 100                              | Caputi et al. (2006)   |
| Local ULIRGs                   | 0.2 - 50.0                             | This work              |

**Table 7.** The stellar masses of the different types of high-z star forming galaxies found in different studies. The stellar masses for the ULIRGs found in this study are also shown in the table for comparison. Note that the upper limit of  $50 \times 10^{10} M_{\odot}$  is found for the radio galaxy PKS1345+12, which represents an exceptional case among the ULIRGs in our sample. All results obtained for the high-z star forming galaxies are based on the modelling of photometric points from the optical to the mid-IR.

Frazer et al. (2004), based on deep near-IR imaging, concluded that the colours, luminosities, morphologies and sizes of the SMGs in their sample are all consistent with the properties of local ULIRGs. Furthermore, on the basis of their CO millimeter observations, Tacconi et al. (2006) conclude that SMGs appear to be the “scaled-up” version of local ULIRGs. Therefore, it is interesting to compare the results of this study with those obtained for high-z star forming galaxies.

Table 7 shows a compilation of the results obtained from various studies of the stellar masses of high-z star forming galaxies. We find that the masses of the local ULIRGs in our sample are, in general, comparable with or slightly higher than, those of the LBGs in the Papovich et al. (2001) sample. In the cases of the SMGs and the DRGs, the results found by Tacconi et al., 2008 and Papovich et al. (2006) are consistent with the total stellar mass estimated in this work for local ULIRGs, and reinforce the idea that the latter objects are the low redshift analogues of the SMGs and DRGs found at higher redshifts. On the other hand, we find that the estimated stellar masses for the ULIRGs in our sample are significantly smaller (with the exception of the radio galaxy PKS12345+12) than many of the *Spitzer* galaxies. This result is consistent with those of the recent studies of, for example, Yan et al. (2007), Sajina et al. (2007),

Sajina et al. (2008), Rigby et al. (2008) and Farrah et al. (2008) among others, suggesting that the *Spitzer* galaxies are either maximum starburst, i.e. scaled-up versions of local ULIRGs, or indeed, represent a separate class of objects from local ULIRGs.

Finally, note that the results obtained for the stellar populations of high-*z* star forming galaxies are based on fits to relatively few photometric points, albeit with a wide spectral range. The modelling work detailed in Paper I emphasized the difficulty in obtaining a unique solution when using combinations of different stellar populations to model spectra, especially on the basis of fits to the SED alone (i.e. not examining the detailed absorption features). We have also shown that some results, and therefore the conclusions based on them, can change significantly with different modeling assumptions. Furthermore, the SED fits for DRGs in the Papovich et al. (2006) sample are relatively poor ( $\chi^2 \gtrsim 2$ ) in a large fraction ( $\gtrsim 50\%$ ) of the sources. Such poor fits would not be accepted as viable in our study of ULIRGs. Clearly, particular care must be taken when interpreting the results obtained on the basis of modelling a few photometric points using combinations of stellar templates, which is often the technique used in high-*z* studies. Studies similar to the one presented here are vital for increase our understanding, not only of the properties of the stellar populations in high-*z* star forming galaxies, but also the nature of the links between these objects and the local ULIRGs.

## 9 SUMMARY AND CONCLUSIONS

In this paper we have presented a detailed analysis of the modelling results presented for the CS and the ES samples in Paper I. In addition, we have also discussed these results in a more general context, comparing them with other studies of ULIRGs. The conclusions can be summarized as follows.

- **Age, reddening and percentage contribution:** we find that the YSPs are more significant in the nuclear than in the extended regions. The statistical analysis presented here suggests that the YSPs located in the nuclear regions tend to be younger and more reddened, although further analysis is required to confirm this result. All of these results are consistent with the merger simulations.

- **Correlations:** we find no evidence for correlations between the properties of the stellar populations and other properties of ULIRGs. This can be explained in terms of a selection effect, i.e. since the objects in the CS and the ES samples are ULIRGs, with high IR-luminosities and star formation rates, it is likely that we are observing them at, or after, the first encounter, or at the end of the merger event, when the nuclei are very close to coalescing. Therefore, they all have similar properties. A second possibility to explain the apparent lack of correlations is the scatter in the properties of the YSPs due to uncertainties in the modelling technique. A third possible explanation is that other variables, such as gas content of the parent galaxies and the geometry of the collision, may have a more important impact on the stellar properties of ULIRGs than the optical spectral classification, interaction class or luminosity.

- **Merger simulations:** in general our modelling results are consistent with the merger simulations, with the IYSPs

in most systems plausibly associated with the first enhancement of activity following the first encounter of the nuclei of the merging galaxies, and the VYSPs likely related to the final enhancement as the nuclei merge together.

- **100 Myr cut-off:** when using Comb I, we find a clear cut-off in luminosity weighted YSP ages at 100 Myr for the nuclear apertures, consistent with the timescale of the merger-induced starburst activity predicted by the merger simulations in the final stages of the merger event, as the nuclei coalesce. This result supports the idea that, despite the varying morphologies, we are observing most of the objects close to the peak of the star formation activity in the final stages of the merger event.

- **The masses of the parent galaxies:** both progenitor galaxies in the trigger events must be in the upper 25% of the mass range of late-type spirals for most of the ULIRGs in the ES.

- **The morphologies of the parent galaxies:** although in most cases the results are consistent with the idea that the progenitors are late-type spirals (albeit unusually massive late-type spirals), in 3 cases (IRAS 13451+1232, IRAS 21208-0519 and IRAS 23327+2913) there is clear evidence that at least one of the progenitors is an early-type galaxy. This demonstrates that ULIRGs can potentially be triggered by mergers between galaxies with a range of galaxy types.

- **Stellar mass content:** our modelling results suggest that most ULIRGs are sub- $m_*$ , or  $m_*$  systems ( $m_* = 1.4 \times 10^{11} M_\odot$ ). Such masses support the idea that these systems will eventually evolve into intermediate mass elliptical galaxies. The masses obtained from the modelling results are generally consistent with the dynamical mass estimates (when available) within a factor of  $\sim 2$ . This result shows that the stellar populations detected in the optical dominate the stellar masses of the galaxies.

- **Bolometric luminosities:** our results suggest that the stellar populations detected at optical wavelengths make a significant contribution to the mid- to far-IR luminosities of many of sources. However, due to uncertainties related to the combination of stellar populations assumed, and to the assumption that all the stellar emission is absorbed by, and heats, the dust, it is possible that the values presented in Table 10 in paper I and Figure 5 in this paper are over-estimates. We conclude that while the visible stellar populations can make a significant contribution to the heating of the dust, it is unlikely that they dominate the heating of the dust in most cases.

- **The evolution of ULIRGs:** the stellar masses of the ULIRGs in the ES sample are consistent with the idea that ULIRGs evolve into intermediate mass elliptical galaxies. On the other hand, the data do not provide any clear evidence to support/refute the evolutionary sequence: cool ULIRG  $\rightarrow$  warm ULIRG  $\rightarrow$  optically selected QSO, since the stellar populations of the cold/warm, Sy/non-Sy, QSO/non-QSO ULIRGs are similar (perhaps the timescale of this transition is shorter than the timescale of the major merger-induced starburst). However, it remains possible that some ULIRGs evolve into radio galaxies (although not all radio galaxies can have this origin).

- **High-*z* counterparts:** many of the properties of the ULIRGs in our sample, such as morphology, stellar mass content, star formation histories etc., are consistent with the

idea that ULIRGs are the local counterparts of the sub-mm galaxies (SMGs) and distant-red galaxies (DRGs).

## ACKNOWLEDGMENTS

We thank the anonymous referee for useful comments that have helped to improve this manuscript. JRZ acknowledges financial support from the STFC in the form of a PhD studentship. JRZ also acknowledges financial support from the spanish grant ESP2007-65475-C02-01. RGD is supported by the Spanish Ministerio de Educación y Ciencia under grant AYA 2007-64712. We also thank support for a joint CSIC-Royal Astronomy Society bilateral collaboration grant. The William Herschel Telescope is operated on the island of La Palma by the Isaac Newton Group in the Spanish Observatorio del Roque de los Muchachos of the Instituto de Astrofísica de Canarias.

## REFERENCES

- Barnes J., Hernquist L., 1996, *ApJ*, 471, 115
- Blain A. W., Smail I., Ivison R. J., Kneib J.-P., Frayer D. T., 2002, *Phys.Rep.*, 369, 111
- Canalizo G., Stockton A., 1997, *ApJ*, 490, L5
- Canalizo G., Stockton A., 2000a, *AJ*, 528, 201
- Canalizo G., Stockton A., 2000b, *AJ*, 120, 1750
- Canalizo G., Stockton A., 2001, *ApJ*, 555, 719
- Caputi K. I., Dole H., Lagache G., McLure R. J., Puget J.-L., Rieke G. H., Dunlop J. S., Le Floch E., Papovich C., Pérez-González P. G., 2006, *ApJ*, 637, 727
- Chapman S. C., Windhorst R., Odewahn S., Yan H., Conselice C., 2003, *ApJ*, 599, 92
- Cole S., Norberg P., Baugh C. M., Frenk C. S., Bland-Hawthorn J., Bridges T., Cannon R., Colless M., Collins C., Couch W., 2001, *MNRAS*, 326, 255
- Colina L., Arribas S., Monreal-Ibero A., 2005, *ApJ*, 621, 725
- Conselice C. J., Blackburne J. A., Papovich C., 2005, *ApJ*, 620, 564
- Cox T. J., Jonsson P., Primack J. R., Somerville R. S., 2006, *MNRAS*, 373, 1013
- Dasyra K., Tacconi L., Davies R., Naab T., Genzel R., Lutz D., Sturm E., Baker A., Veilleux S., Sanders D., Burkert A., 2006a, *ApJ*, 638, 745
- Dasyra K., Tacconi L., Davies R., Naab T., Genzel R., Lutz D., Sturm E., Baker A., Veilleux S., Sanders D., Burkert A., 2006b, *ApJ*, 651, 835
- Dasyra K. M., Tacconi L. J., Davies R. I., Genzel R., Lutz D., Peterson B. M., Veilleux S., Baker A. J., Schweitzer M., Sturm E., 2007, *ApJ*, 657, 102
- di Matteo P., Combes F., Melchior A.-L., Semelin B., 2007, *A&A*, 468, 61
- Erb D. K., Shapley A. E., Steidel C. C., Pettini M., Adelberger K. L., Hunt M. P., Moorwood A. F. M., Cuby J.-G., 2003, *ApJ*, 591, 101
- Erb D. K., Steidel C. C., Shapley A. E., Pettini M., Adelberger K. L., 2004, *ApJ*, 612, 122
- Evans A., Mazzarella J., Surace J., Sanders D., 2002, *AJ*, 580, 749
- Farrah D., Afonso J., Efstathiou A., Rowan-Robinson M., Fox, M. Clements D., 2003, *MNRAS*, 343, 585
- Farrah D., Lonsdale C. J., Weedman D. W., Spoon H. W. W., Rowan-Robinson M., Polletta M., Oliver S., Houck J. R., Smith H. E., 2008, *ApJ*, 677, 957
- Farrah D., Rowan-Robinson M., Oliver S., Serjeant S., Borne K., Lawrence A., Lucas R. A., Bushouse H., Colina L., 2001, *MNRAS*, 326, 1333
- Franx M., Labbé I., Rudnick G., van Dokkum P. G., Daddi E., Förster Schreiber N. M., Moorwood A., Rix H.-W., Röttgering H., van de Wel A., van der Werf P., van Starckenburg L., 2003, *ApJ*, 587, L79
- Frayer D. T., Reddy N. A., Armus L., Blain A. W., Scoville N. Z., Smail I., 2004, *AJ*, 127, 728
- Genzel R., Tacconi L. J., Rigopoulou D., Lutz D., Tecza M., 2001, *ApJ*, 563, 527
- Gialvalisco M., 2002, *ARA&A*, 40, 579
- Heckman T. M., Kauffmann G., Brinchmann J., Charlot S., Tremonti C., White S. D. M., 2004, *ApJ*, 613, 109
- Kauffmann G., White S. D. M., Heckman T. M., Ménard B., Brinchmann J., Charlot S., Tremonti C., Brinkmann J., 2004, *MNRAS*, 353, 713
- Kennicutt R., 1998, *ARA&A*, 36, 189
- Kim D. C., Sanders D. B., 1998, *ApJ*, 119, 41
- Mihos J., Hernquist L., 1996, *ApJ*, 464, 641
- Mirabel I., Sanders D., 1988, *ApJ*, 355, 104
- Papovich C., Dickinson M., Ferguson H. C., 2001, *ApJ*, 559, 620
- Papovich C., et al. 2004, *ApJS*, 154, 70
- Papovich C., et al. 2006, *ApJ*, 640, 92
- Pope A., Borys C., Scott D., Conselice C., Dickinson M., Mobasher B., 2005, *MNRAS*, 358, 149
- Rigby J. R., Marcellac D., Egami E., Rieke G. H., Richard J., Kneib J.-P., Fadda D., Willmer C. N. A., Borys C., van der Werf P. P., Pérez-González P. G., Knudsen K. K., Papovich C., 2008, *ApJ*, 675, 262
- Roberts M., Haynes M., 1994, *ARA&A*, 32, 115
- Robinson T., Tadhunter C., Axon D., Robinson A., 2000, *MNRAS*, 317, 922
- Rodríguez Zaurín J., Holt J., Tadhunter C., González Delgado R., 2007, *MNRAS*, 375, 1133
- Rodríguez Zaurín J., Tadhunter C. N., González Delgado R. M., 2008, *MNRAS*, 384, 875
- Sajina A., Yan L., Armus L., Choi P., Fadda D., Helou G., Spoon H., 2007, *ApJ*, 664, 713
- Sajina A., Yan L., Lutz D., Steffen A., Helou G., Huynh M., Frayer D., Choi P., Tacconi L., Dasyra K., 2008, *ApJ*, in press, astro
- Sanders D. B., Mirabel I. F., 1996, *ARA&A*, 34, 749
- Sanders D. B., Soifer B. T., Elias J. H., Madore B. F., Matthews K., Neugebauer G., Scoville N. Z., 1988, *ApJ*, 325, 74
- Sanders D. B., Soifer B. T., Elias J. H., Neugebauer G., Matthews K., 1988, *ApJ*, 328, L35
- Smail I., Ivison R. J., Blain A. W., Kneib J.-P., 2002, *MNRAS*, 331, 495
- Solomon P., Downes D., Radford S., Barret J., 1997, *ApJ*, 478, 144
- Springel V., Di Mateo T., Hernquist L., 2005, *MNRAS*, 361, 776
- Surace J., Sanders D., Evans A., 2000, *ApJ*, 529, 170
- Surace J. A., Sanders D., 2000, *ApJ*, 120, 604

- Surace J. A., Sanders D. B., Vacca W. D. Veilleux S., Mazarella J. M., 1998, ApJ, 492, 116
- Surace J. A., Sanders D. C., 1999, ApJ, 512, 162
- Tacconi L., et al. 2008, ApJ, accepted, astro
- Tacconi L. J., Genzel R., Lutz D., Rigopoulou D., Baker A. J., Iserlohe C., Tecza M., 2002, ApJ, 580, 73
- Tacconi L. J., Neri R., Chapman S. C., Genzel R., Smail I., Ivison R. J., Bertoldi F., Blain A., Cox P., Greve T., Omont A., 2006, ApJ, 640, 228
- Tadhunter C., Dicken D., Holt J., Inskip K., Morganti R., Axon D., Buchanan C., González Delgado R., Barthel P., van Bemmel I., 2007, ApJ, 661, L13
- Tadhunter C., Dickson R., Morganti R., Robinson T., Wills K., Villar-Martin M., Hughes M., 2002, MNRAS, 330, 977
- Tadhunter C. N., Robinson T. G., González Delgado R. M., Wills K., Morganti R., 2005, MNRAS, 356, 480
- Wills K. A., Morganti R., Tadhunter C. N., Robinson T. G., Villar-Martin M., 2004, MNRAS, 347, 771
- Wills K. A., Tadhunter C. N., Holt J., González Delgado R. M., Rodríguez-Zaurín J., Morganti R., 2008, MNRAS, accepted for publication
- Yan L., Sajina A., Fadda D., Choi P., Armus L., Helou G., Teplitz H., Frayer D., Surace J., 2007, ApJ, 658, 778
- Young J., Knezek P., 1989, ApJ, 347, L55